Design of Operation Parameters to Resolve Two Targets using Proximity Sensors

Qiang Le
Department of Electrical Engineering
Hampton University
Hampton, VA, U.S.A.
qiang.le@hamptonu.edu

Lance M. Kaplan
US Army Research Laboratory
Adelphi, MD, U.S.A.
lkaplan@ieee.org *

Abstract − *This work provides a design method to achieve a specified probability of resolution for two target localization via a wireless network of proximity sensors. Proximity sensors simply report a single binary value indicating whether or not a target is near. The design provides the density and threshold settings to achieve the given probability of resolution for targets separated by a specified distance. Simulations are included that demonstrate that at the designed sensor density and threshold values, the actual percentage of targets resolved achieves the desirable level of resolution for moderate to large target separations.*

Keywords: wireless sensor networks, source localization, binary sensors, maximum likelihood estimation

1 Introduction

Proximity (or binary) sensors are simple devices that report whether or not they detect an object. A binary sensor can consist of a passive device such as an acoustic microphone where it reports a detection when the energy of the signal computed over an integration period exceeds a threshold. In essence, it acts as a tripwire sensor. These sensors have proved useful in a number of applications where they cue more expensive devices to interrogate the scene using a more expensive and informative sensor upon detection. This paper investigates the feasibility of a network of proximity sensors to localize targets. In such a network, the no detection report is as valuable as a detection report. Previous work has revealed the potential of target localization via a mesh network of proximity sensors by proposing localization methods for the single target case [1, 2, 3, 4, 5, 6]. Recent work presents maximum likelihood (ML) localization algorithms for multi-target localization when the number of targets is known *a priori* [7]. When the number of targets is not known *a priori*, the finite-set based Probability Hypothesis Density (PHD) filter [8], which can provide reasonable estimates of the number of targets and the target states, might prove useful for proximity sensors. To understand the feasibility of any proximity-based localization method, one needs to develop fundamental performance bounds that determine how well a network of proximity sensors can localize targets given the operation parameters of the sensor network. Here, the operation parameters include the density of the sensor nodes and the threshold settings for the sensors.

To localize targets effectively, one must be able to resolve them. To the best of our knowledge, the notion of target resolution has not been investigated for a proximity sensor network. This paper presents our initial work to understand target resolution for such networks, and to determine the operation parameters to achieve resolution of targets separated by a specified distance. To this end, the work exploits a physically justifiable sensor model that determines the probability of detecting targets based upon the location of the targets relative to each sensor. As an initial investigation, a number of simplifying assumptions are made such as the location of all sensor nodes are known exactly, the power of radiation from all target sources are equal and known, the propagation loss exponent is known, no communications errors, perfect time synchronization, etc. Once the fundamental performance bounds for the simplified case is developed, the assumptions can be relaxed. Finally, the analysis in the paper assumes that the mesh network is developed by tossing out the sensor nodes randomly so that they distribute via a statistical uniform distribution over the coverage area. Other work can investigate performance bounds when the sensors are intentionally placed to achieve op-

*Research was sponsored by the Army Research Laboratory and was accomplished under Cooperative Agreement Number W911NF-09-2-0041. The views and conclusions contained in this document are those of the authors and should not be interpreted as representing the official policies, either expressed or implied, of the Army Research Laboratory or the U.S. Government. The U.S. Government is authorized to reproduce and distribute reprints for Government purposes notwithstanding any copyright notation herein.

timal performance.

The paper is as organized as follows. Section 2 provides details about the sensor model, and Section 3 discusses the ML localization method and demonstrates how the likelihood surfaces can resolve two targets under various conditions. Section 4 uses the insight from the previous section to devise a strategy to design the operational parameters so that the desired level of target resolution can be achieved. The effectiveness of the design strategy is investigated via simulations in Section 5. Finally, Section 6 provides concluding remarks.

2 Sensor Model

This section provides the sensor model for proximity sensors that has been incorporated in earlier work [6, 9]. The received power p_i^t, i.e., the power measurement of the i-th sensor at time t, is given by

$$p_i^t = \sum_{k=1}^{K} p_{0,k}^t \left(\frac{r_{0,k}}{r_{i,k}^t} \right)^{\alpha} + v_i^t, \tag{1}$$

where $p_{0,k}^t$ is the power measured at a reference distance $r_{0,k}$ for the k-th target, K is the total number of targets, $r_{i,k}^t$ is the relative distance between the i-th sensor and the k-th target, α is the attenuation parameter that depends on the transmission medium, and

$$v_i^t \sim \mathbf{N}\left(\mu_v, \sigma_v^2\right).$$

The mean and variance of the error v_i^t is derived from the zero mean measurement noise of variance σ^2 for the case that the measured power is the result of integrating the square of the measurements over L samples. As shown in [6, 9], $\mu_v = \sigma^2$ and $\sigma_v^2 = 2\sigma^4/L$. This paper assumes the references $r_{0,k} = r_0$ and $p_{0,k} = p_0$ for all K targets, and r_0 and p_0 are known.

The i-th sensor measures the received power p_i^t, processes it locally and reports a single binary digit: '1' for the presence of one or more targets or '0' for the absence of any target. The decision follows the rule

$$d_i^t = \begin{cases} 1 & p_i^t > \lambda, \\ 0 & p_i^t \leq \lambda. \end{cases} \tag{2}$$

Given a probability of false alarm P_{fa}, the threshold λ is computed as:

$$\lambda = \sigma_v Q^{-1}(P_{fa}) + \mu_v, \tag{3}$$

where $Q(\cdot)$ is the Q-function

$$Q(x) = \frac{1}{\sqrt{2\pi}} \int_x^{\infty} e^{-\frac{t^2}{2}} dt.$$

Furthermore, the probability of detection P_d at the i-th sensor, for a given threshold (or P_{fa}), as a function of the distances to the k targets, is

$$\begin{aligned} P_d(\mathbf{r}_i^t) &= \text{Prob}(d_i^t = 1 | \text{targets}), \\ &= \text{Prob}(p_i^t > \lambda | \text{targets}), \\ &= Q\left(\frac{\lambda - \sum_{k=1}^{K} p_{0,k}^t \left(\frac{r_{0,k}^t}{r_{i,k}^t} \right)^{\alpha} - \mu_v}{\sigma_v} \right), \end{aligned} \tag{4}$$

where $\mathbf{r}_i^t = \left[r_{i,0}^t, \ \ldots, \ r_{i,k}^t \right]$. Fig. 1 illustrates P_d as a function of the distance of a single target to a sensor. The figure demonstrates that P_d as given by (4) behaves as a sigmoid function that steps down from a value near one to a value near P_{fa} over a transition region of about 200 meters.

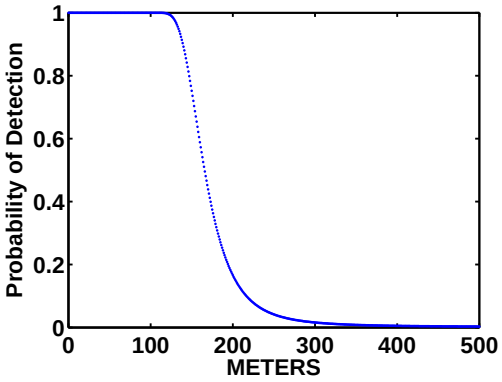

Figure 1: P_d vs. the distance, where P_{fa}=0.001, $\alpha = 2$, $\sigma = 0.5$, $p_0 = 3000$, $r_0 = 1$m, and $L = 100$.

3 Maximum Likelihood Localization

The single target ML localization algorithm for binary sensors was devised in [2] and further explored in [4]. The likelihood is the probability of the observed measurements for the N sensors, i.e, d_i^t for $i = 1, \ldots, N$, conditioned on the location of the targets x_k for $k = 1, \ldots, K$ and the location of the sensor nodes S_i for $i = 1, \ldots, N$. Thus, the K-target likelihood function is given by

$$\begin{aligned} &\prod_{i=1}^{N} \left(P_d\left([|x_1 - S_i|, \ldots, |x_K - S_i|] \right) \right)^{d_i^t} \cdot \\ &\cdot \left(1 - P_d\left([|x_1 - S_i|, \ldots, |x_K - S_i|] \right) \right)^{(1 - d_i^t)}. \end{aligned} \tag{5}$$

One can maximize (5) to obtain the K estimated target positions, which are ML estimates [7]. For the case that $K = 1$, (5) simplifies to the 1-target likelihood function as originally described in [2].

The ML target location estimates are obtained by using a hill climbing algorithm to maximize (5). Because the likelihood surface may have multiple peaks,

it is important to initialize the hill climbing algorithm with a good initial guess for the target locations. Our previous work in [7] considers three practical initialization approaches: 1) centroid of k-means, 2) centroid of largest two maximal cliques, and 3) peak in 1-target likelihood surface.

The first two initialization methods employ clustering approaches; namely, k-means clustering and clique clustering. In general, both methods cluster the sensor detections in K classes associated to the known K number of targets. The first approach employs the k-means algorithm by clustering based on the geographic positions of the nodes reporting detections and returns the K centroids as the initial target position estimates. On the other hand, the maximal clique approach first creates a graph of the nodes returning detections where edges exist between nodes when they are both able to detect a common target at sufficient P_d. Then, it finds K maximal cliques under the assumption that each clique is generated from a different target. Finally, it computes the centroid associated to the node positions from the K cliques as the initial estimates of the target position.

Unlike the first two methods, the 1-target likelihood surface does not assume any association between the sensor detections and the targets. However, it is computationally complex. It first assumes one target, i.e., $K = 1$ and calculates the one-target likelihood of the target position over a uniform grid of points by (5). Note that the largest peaks on the surface should correspond to the true target locations. Because it is impossible to visualize the general K-target likelihood surface when $K > 1$, the 1-target likelihood surface provides a convenient means to investigate how sensor placement can affect the ability to resolve targets. To this end, two targets are considered resolved when the two peaks closest to the ground truth target positions are the two largest peaks in the likelihood map.

Fig. 2 shows the likelihood surface for two targets separated by $r_s = 600$m. The bright regions are either due to the possible target locations or no sensor coverage, and the dark blue disk regions are due to sensors reporting 'no targets'. Figs. 2(a) and (c) show the physical configuration of the targets (the red pluses), the nodes that do not detect targets (the blue dots), and the nodes that do detect a target (the larger green faced circles). Figs. 2(b) and (d) show the likelihood surfaces with white pluses as cues for the target locations. In Figs. 2(a) and (b), no sensors report target locations and small peaks occur in the likelihood surface at locations beyond the detection range of the sensors. In Figs. 2(c) and (d), two sensors do detect the targets, but the resulting peaks in the likelihood surface are modest because the nearby sensors that do not detect the targets provide evidence against the existence of any targets. In either case, the sensor network geometry is unable to resolve the two targets.

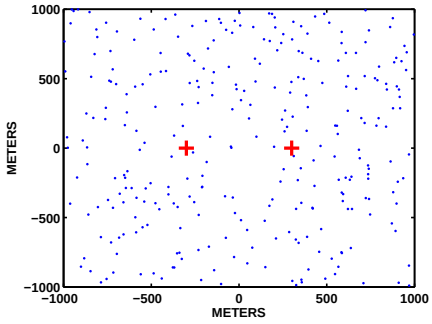

(a)

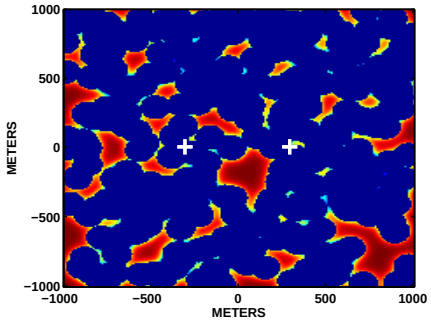

(b)

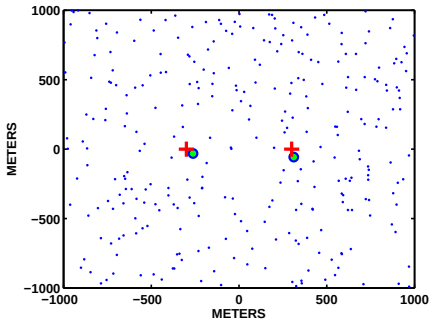

(c)

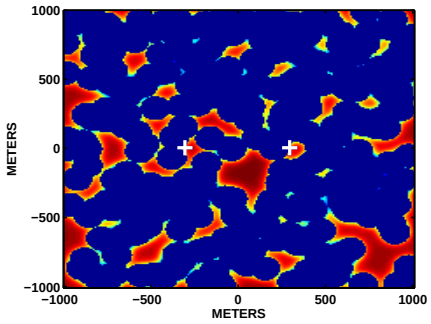

(d)

Figure 2: Demonstration of the ability of the 1-target likelihood surface to resolve two targets separated by 600m: (a) The collection geometry where no sensors report detections, (b) the corresponding likelihood surface, (c) the collection geometry when two closest sensors report detections, and (d) the corresponding likelihood surface.

Fig. 3 shows the likelihood surface for two targets that are even closer than in Fig. 2; namely, $r_s = 300$m. In Fig. 3(a) most of the nodes within detection range of the targets do detect the target. The corresponding likelihood surface demonstrates a broad peak that covers both targets, and the targets are not resolved. In Fig. 3(c), a sensor that lies between the two targets does not report a detection. In that case, this "between" node is able to cut the peak in Fig. 3(b) into two peaks in Fig. 3(d), and the two targets are resolved. Overall, Figs. 2 and 3 demonstrate that to resolve the targets, most of the sensors near the targets must report detections and a "between" sensor must report no detection. This insight leads to a proximity sensor network design strategy as reported in the next section.

4 Design of Operation Parameters

Inspection of the likelihood surfaces reveals the conditions necessary for the network of proximity sensors to resolve two targets. Two targets are resolved when the two largest peaks in the likelihood surface correspond to the location of the targets. Because it is impossible to visualize the 2-target likelihood surface, we use the analysis of the 1-target likelihood surface to dictate the conditions necessary to achieve target resolution. As revealed in Section 3, two targets separated by r_s meters can be resolved when 1) at least one sensor is close enough to each target to detect it, 2) most of the sensors that can detect a target actually report a detection, and 3) there exist a sensor between the targets that is sufficiently far from either target to report a detection. The first two conditions can be achieved by various combinations of threshold and sensor density settings. By lowering the threshold, a smaller node density can achieve the first two conditions. However, the third condition provides a lower bound for the threshold so that the "between" sensor cannot detect target.

The section provides the design criteria to obtain a specified probability of resolution P_r at a specified target separation distance r_s. This criteria is for the case that the sensor nodes are uniformly distributed over its coverage area so that the node locations approximate a realization of a Poisson Point Process (PPP) [10]. Based on the conditions of target resolution, the probability of resolution P_r can be bounded by

$$P_r \geq (\tau_1 \tau_2)^2 (1 - \tau_3), \tag{6}$$

where τ_1 is the lower bound probability that a sensor within range r to the target can detect it, τ_2 is the probability that at least one sensor is within range r and τ_3 is the probability that the "between" sensor reports a detection. Because the first two conditions must be met for both targets, τ_1 and τ_2 are squared in (6).

Actually, $\tau_1 \tau_2$ is an approximation for the lower bound for the first two conditions to be met at a single

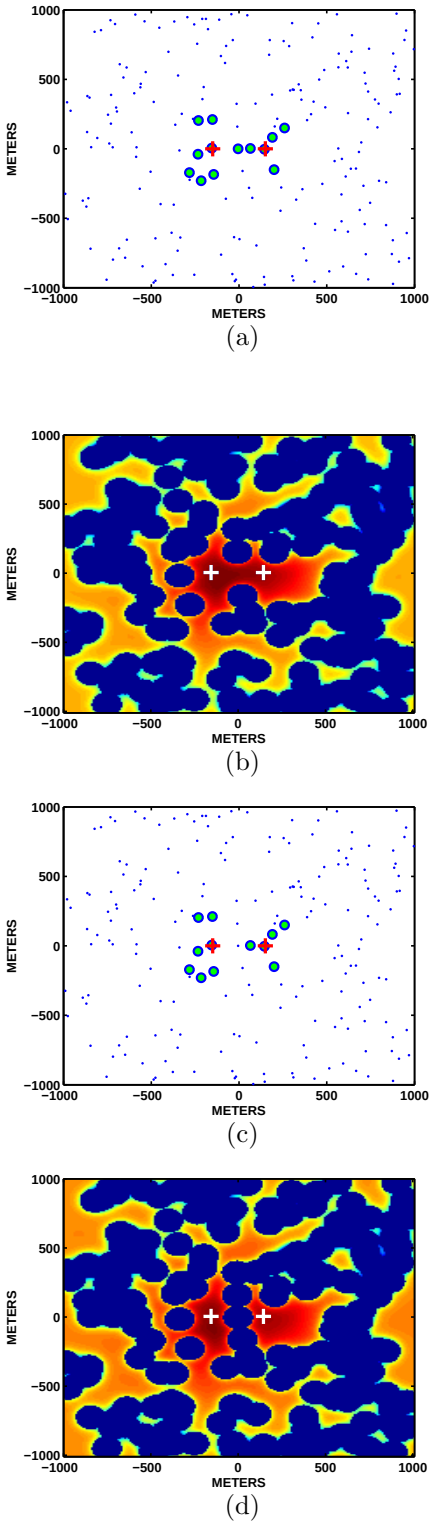

Figure 3: Demonstration of the ability of the 1-target likelihood map to resolve two targets separated by 300m: (a) The collection geometry where 13 sensors report detections, (b) the corresponding likelihood surface, (c) the collection geometry where 12 sensors report detections while the "between" sensor reports 'no detection', and (d) the corresponding likelihood surface.

target. By definition,

$$\tau_1 = Q\left(\frac{\lambda - \frac{p_0 r_0^\alpha}{r^\alpha} - \mu_v}{\sigma_v}\right) \quad (7)$$

since by (4), P_d is larger for targets closer than range r. Furthermore, for a given sensor density ρ of the PPP [11, 12]

$$\tau_2 = 1 - \exp(-\pi\rho r^2). \quad (8)$$

Note that $\rho = N/A$, where N is the number of sensor nodes within the network and A is the area covered by sensor network. Now, if we treat τ_1 as the probability of detection for all nodes within range r to the target, then the nodes that report a detection and do not report a detection form PPPs whose densities are $\tau_1\rho$ and $(1-\tau_1)\rho$, respectively [10]. Thus, within the circular region of radius r around the target, the probability that at least one node reports a detection is given by

$$p_1 = 1 - \exp(-\rho\tau_1\pi r^2). \quad (9)$$

Furthermore, the probability that all nodes within the circular region report a detection is

$$\begin{aligned} p_a &= p_1 \exp(-\rho(1-\tau_1)\pi r^2), \quad (10)\\ &= \exp(-\rho(1-\tau_1)\pi r^2) - \exp(-\rho\pi r^2). \end{aligned}$$

The probability that most sensors within the circular region detect the target is bounded below by p_a and above by p_1. As shown in the Appendix,

$$p_a \le \tau_1\tau_2 \le p_1. \quad (11)$$

As τ_1 increases to one, the bounds in (11) become tight. Hence, $\tau_1\tau_2$ is a reasonable proxy for the probability that the first two conditions of resolvability are met for a single target.

For a given value of τ_2, the achievable node density as a function of the detection range that achieves a P_d of at least τ_1 is given by

$$\rho = -\frac{\ln(1-\tau_2)}{\pi r^2}, \quad (12)$$

where by the inverse of (7)

$$r = \frac{p_0^{\frac{1}{\alpha}} r_0}{(\lambda - \sigma_v Q^{-1}(\tau_1) - \mu_v)^{\frac{1}{\alpha}}}. \quad (13)$$

Thus, the relationship between achievable ρ and parameters τ_1 and τ_2 is

$$\rho = -\frac{\ln(1-\tau_2)}{\pi p_0^{\frac{2}{\alpha}} r_0^2}(\lambda - \sigma_v Q^{-1}(\tau_1) - \mu_v)^{\frac{2}{\alpha}}. \quad (14)$$

To meet the first two resolvability conditions for a given τ_1 and τ_2, the node density can be made smaller by simply decreasing the threshold λ, i.e., increasing the effective detection range of the sensors. However, the threshold cannot be made arbitrarily small or else the final resolvability condition cannot be met. To meet the final condition, the probability that the "between" sensor reports a detection is

$$\tau_3 = Q\left(\frac{\lambda - \frac{2p_0 r_0^\alpha}{(0.5r_s)^\alpha} - \mu_v}{\sigma_v}\right). \quad (15)$$

Thus, the threshold cannot be smaller than

$$\lambda = \sigma_v Q^{-1}(\tau_3) + \frac{2p_0 r_0^\alpha}{(0.5r_s)^\alpha} + \mu_v, \quad (16)$$

and insertion of (16) into (14) leads to the smallest achievable node density ρ_c for given values of τ's, i.e.,

$$\rho_c = -\left(\sigma_v(Q^{-1}(\tau_3) - Q^{-1}(\tau_1)) + \frac{2p_0 r_0^\alpha}{(0.5r_s)^\alpha}\right)^{\frac{2}{\alpha}} \frac{\ln(1-\tau_2)}{\pi p_0^{\frac{2}{\alpha}} r_0^\alpha}. \quad (17)$$

Judicious selection of the $\tau' s$ can provide a small critical density. For the P_r specification, (6) leads to two degrees of freedom for the τ's, where by considering arbitrary τ_1 and τ_2, $\tau_3 = 1 - \frac{P_r}{(\tau_1\tau_2)^2}$. A good design should determine the smallest ρ_c. For this reason, the sensor network design minimizes (17) to obtain the critical sensor density:

$$\rho_c^* = \rho_c(\tau_1^*, \tau_2^*), \quad (18)$$

where

$$\{\tau_1^*, \tau_2^*\} = \arg\min_{\tau_1,\tau_2} \rho_c(\tau_1, \tau_2). \quad (19)$$

Inspection of (17) over a grid of admissible values of τ_1 and τ_2 indicates that there is a unique minimum. Future work will try to prove this claim. We determine ρ_c^* using the Nelder-Mead simplex algorithm via the `fminsearch` function in Matlab. The search is initialized by setting $\tau_1 = \tau_2 = \sqrt[5]{P_r}$.

Overall, to achieve a probability of resolution of P_r for two targets separated by a distance of r_s using a proximity sensor network covering an area of A, one must use $N_c = \rho_c^* A$ sensors with a threshold setting of

$$\lambda^* = \sigma_v Q^{-1}\left(1 - \frac{P_r}{(\tau_1^*\tau_2^*)^2}\right) + \frac{2p_0 r_0^\alpha}{(0.5r_s)^\alpha} + \mu_v. \quad (20)$$

Equivalently, by (3), the P_{fa} for the sensor node designed to be

$$P_{fa}^* = Q\left(Q^{-1}\left(1 - \frac{P_r}{(\tau_1^*\tau_2^*)^2}\right) + \frac{2p_0 r_0^\alpha}{\sigma_v(0.5r_s)^\alpha}\right). \quad (21)$$

The proximity sensor network design is accomplished via (17)-(21).

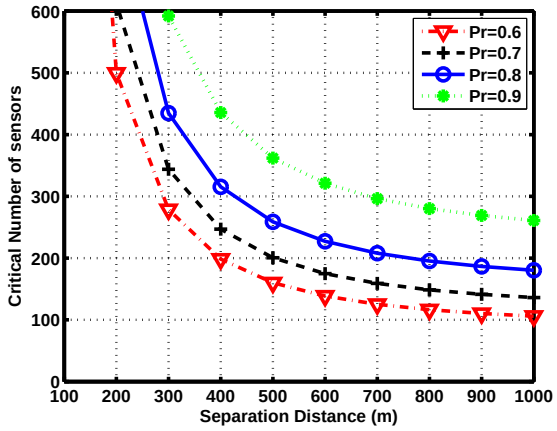

Figure 4: Critical number of sensors versus specified r_s for various specified values of P_r using (17).

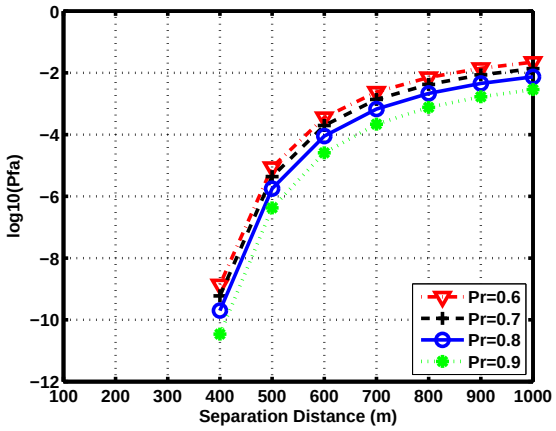

Figure 5: Critical P_{fa} versus specified r_s for various specified values of P_r using (21)

5 Simulations

This section provides simulations when the propagation loss factor is $\alpha = 2$, the target power is $p_0 = 3000$ at a normalized distance of $r_0 = 1$m, the ambient noise is $\sigma = 0.5$, and the number of integrated samples is $L = 100$. Furthermore, the sensor field covers a 2km $\times$ 2km region so that $A = 4\text{km}^2$. Fig. 4 shows the theoretical critical number of sensors, i.e., the minimum of (17) via `fminsearch` multiplied by A, as a function of the specified separation distance r_s for various specified values of P_r. As expected, the critical number of sensors decreases as the separation distance increases. Fig. 5 shows the corresponding critical P_{fa} for the given design specifications as given by (21). For a given P_r, as the separation distance decreases, the P_{fa} must decrease, i.e., the threshold increases, so that the "between" sensor does not detect either target. For a given r_s, as P_r increases, more senors are required, and the P_{fa} decreases slightly due to the increase in sensor density. Note that for $r_s < 400$, the P_{fa} is too small to be computed due to the numerical precision of the computer. However, the corresponding thresholds λ are finite.

To prove that the range of P_{fa} and the critical sensor density work to meet the desirable P_r at a specified r_s, we ran 5000 Monte Carlo experiments composed of 100 random sensor network configurations $\times$ 50 Monte Carlo runs per sensor network configuration. In each configuration, the sensors are randomly placed in the 2km $\times$ 2km field via a uniform distribution. The number of nodes placed in the network and their corresponding threshold (or P_{fa}) settings were based on the design criteria as given by (17)-(21). These values are provided in Figs. 4 and 5. For each Monte Carlo realization, we compute the one-target likelihood surface over the whole region. In the one-target likelihood map, the two targets are considered resolved when the two peaks closest to the ground truth target positions are the two largest peaks. The results of the actual percentage of targets resolved are shown in Fig. 6. It is clear that the actual percentage of resolved targets exceed the specified P_r when the targets are separated by more than 600m. The designs are conservative as the achievable probability of resolution should exceed the specified P_r because of (6). When the targets are separated by 400m, the actual P_r is lower than expected when the desired $P_r = 0.8$ or $P_r = 0.9$. This may be due to the fact that the specification of τ_3 in Section 4 only provides the desired false alarm rate of the "between" sensors and does not actually ensure the existence of such a "between" node. At the lower target separations the area for the "between" sensor to exists becomes too small to be accommodated by the critical density that achieves the first two resolvability conditions.

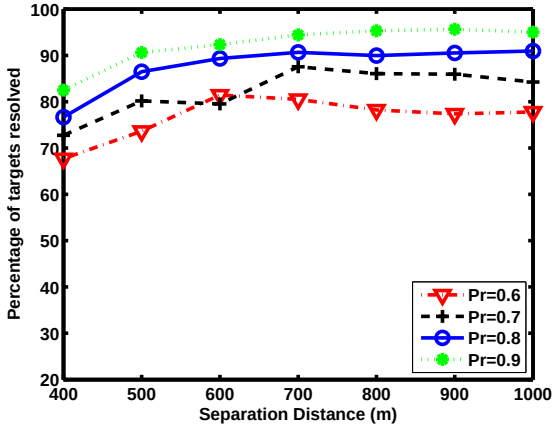

Figure 6: Percentage of targets resolved when the sensor density is ρ_c^* and the thresholds are set to achieve a probability of false alarm of p_{fa}^*.

Finally, we evaluated the ML localization method when the sensor network is designed via the resolvability criteria. Specifically, we ran the ML estimators with various practical initialization methods: centroid of cliques, centroid of k-means, and peaks in the 1-target likelihood surface. We also ran the ML estimator using the ground truth initialization as the performance bound. Then, we determined the percentage of times that the practical initialization methods are able to provide an estimate that is comparable to ground truth initialization method. Fig. 7 shows the percentage of times the ML estimates due to the ground truth initialization agreed with the ML estimates due to one of the practical initialization methods. For most of the time, the correspondence to the ground truth initialization meets or exceeds the specified P_r when the target separation is greater than 500m for the clique and 1-target likelihood methods. For $r_s \leq 500$m, the ground truth correspondence drops similar to the drop in achievable P_r as seen in Fig. 6. When using the k-means for initialization, the ground truth correspondence does not achieve the specified P_r for most cases when $P_r \geq 0.8$.

6 Conclusion

This work documents our initial attempt to determine the operating parameters of a proximity sensor network to achieve a specified probability of resolution at a specified target separation r_s. The probability of resolution is derived by considering three necessary conditions to resolve two target. These conditions consist of 1) node proximity to the targets, 2) sufficient number of detections from nodes close to the target, and 3) the existence of the "between" node that cannot detect either target. These conditions lead to a design strategy that determines the necessary sensor density and threshold settings to achieve the desired P_r for a given r_s. Simulations demonstrate that the design strategy exceeds the specified P_r when $r_s \geq 500$m. For lower values of r_s, the realized P_r can be lower than specified. This may be due to the fact that the design does not consider whether the node density is high enough for the "between" sensor to exist with sufficiently high probability. In other words, the design method assumes that a node at the midpoint of the two targets cannot detect either target. However, it does not factor into account the probability that the node will actually lie near this midpoint.

Future work will revise the design criteria to still achieve the desired P_r when the target separation is small. This may be accomplished by factoring in the probability that a "between" sensor node exist. Furthermore, we plan to investigate methods to predict the root mean squared position error performance of the ML localization estimate. Finally, the simplifying assumptions can be relaxed to obtain performance bounds under ever increasing realistic conditions.

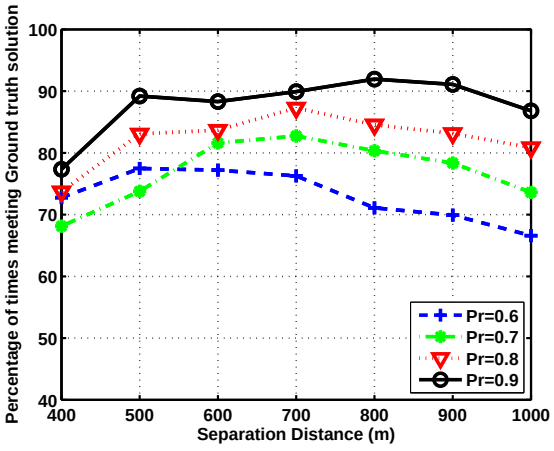

(a)

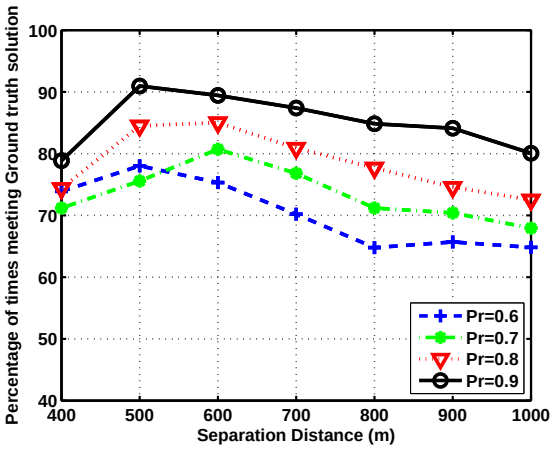

(b)

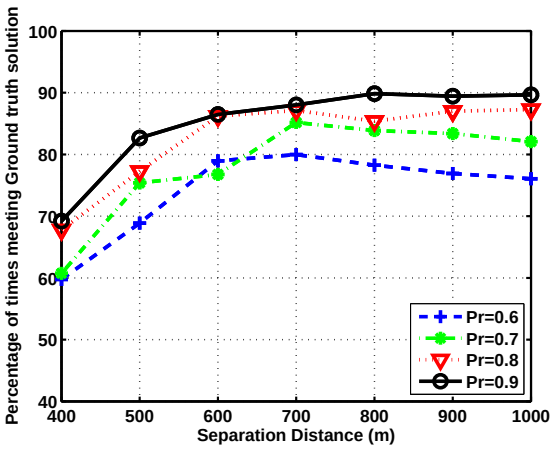

(c)

Figure 7: Percentage of times the practical initialization leads to an ML estimate that corresponds to the ML estimate when initializing by the ground truth: (a) Clique initialization, (b) k-means initialization, and (c) 1-target likelihood initialization.

A Proof for the Inequalities in (11)

Let $a = \exp(-\rho\pi r^2)$. Note that a is bounded by $0 \leq a \leq 1$. Then by considering (8), the bounds in (11) can be expressed as

$$a^{1-\tau_1} - a \leq \tau_1(1-a) \leq 1 - a^{\tau_1}. \tag{22}$$

Since τ_1 corresponds to the probability of detection, it's bounded by $0 \leq \tau_1 \leq 1$. Let's define a function of τ_1 as

$$f(\tau_1) = a^{1-\tau_1} - a - \tau_1(1-a). \tag{23}$$

Clearly $f(0) = f(1) = 0$. The second derivative of $f(\cdot)$ with respect to τ_1 is

$$\frac{d^2 f}{d^2 \tau_1} = (\ln(a))^2 a^{1-\tau_1} \geq 0. \tag{24}$$

Thus, the function is convex, which means that

$$\begin{aligned} f(\tau_1) &\leq (1-\tau_1)f(0) + \tau_1 f(1), \\ &\leq 0, \end{aligned} \tag{25}$$

and

$$a^{1-\tau_1} - a \leq \tau_1(1-a). \tag{26}$$

This proves the first inequality in (22). Similarly, we can define a function of τ_1 as

$$f(\tau_1) = \tau_1(1-a) - 1 + a^{\tau_1}. \tag{27}$$

Clearly, $f(0) = f(1) = 0$ Furthermore the second derivative of $f(\cdot)$ with respect to τ_1 is

$$\frac{d^2 f}{d^2 \tau_1} = (\ln(a))^2 a_1^{\tau} \geq 0. \tag{28}$$

Again the function is convex, and

$$\begin{aligned} f(\tau_1) &\leq (1-\tau_1)f(0) + \tau_1 f(1), \\ &\leq 0. \end{aligned} \tag{29}$$

Thus,

$$\tau_1(1-a) \leq 1 - a^{\tau_1}, \tag{30}$$

which proves the second inequality in (22). ■

References

[1] J. Aslam, Z. Butler, F. Constantin, V. Crespi, G.Cybenko, and D. Rus, "Tracking a moving object with a binary sensor network," in *Proceedings of ACM SensSys*, 2003.

[2] A. Artes-Rodriguez, M. Lazaro, and L. Tong, "Target location estimation in sensor networks using range information," in *IEEE Sensor Array and Multichannel Signal Processing workshop*, 2004.

[3] N. Shrivastava, R. Mudumbai, U. Madhow, and S. Suri, "Target tracking with binary proximity sensors: Fundamental limits, minimal descriptions, and algorithms," in *Proceedings of ACM SensSys*, 2006.

[4] A. Capponi, L. Kaplan, and C. Pilotto, "Performance characterization of random proximity sensor networks," in *Asilomar Conference on Signals, Systems and Computers*, 2006.

[5] J. Singh, U. Madhow, R. Kumar, S. Suri, and R. Cagley, "Tracking multiple targets using binary proximity sensors," in *Proceedings of IPSN*, 2007.

[6] P. Djuric, M. Vemula, and M. Bugallo, "Target tracking by particle filtering in binary sensor networks," *IEEE Trans. on Signal Processing*, vol. 56, no. 6, pp. 2229–2238, 2008.

[7] Q. Le and L. M. Kaplan, "Target localization using proximity binary sensors," in *Proc. of the IEEE Aerospace Conference*, Big Sky, MT, Mar. 2010.

[8] R. Mahler, "Multi-target bayes filtering via first-order multi-target moments," *IEEE Trans. on Aerospace and Electronic Systems*, vol. 39, no. 4, pp. 1152–1178, 2003.

[9] X. Sheng and Y. H. Hu, "Maximum likelihood multiple-source localization using acoustic energy measurements with wireless sensor networks," *IEEE Trans. on Signal Processing*, vol. 53, no. 1, pp. 44–53, 2005.

[10] S. M. Ross, *Introduction to Probability Models*, 8th ed. San Diego, CA: Academic Press, 2003.

[11] C. Bettstetter, "On the minimum node degree and connectivity of a wireless multihop network," in *MOBIHOC*, EPF Lausanne, Switzerland, 2002.

[12] V. Cevher and L. Kaplan, "Acoustic sensor network design for position estimation," *ACM Transactions on Sensor Networks*, vol. 4, 2009.